Catalysis Today 285 (2017) 104–113

Contents lists available at ScienceDirect

Catalysis Today

journal homepage: www.elsevier.com/locate/cattod

Screening the bulk properties and reducibility of Fe-doped Mn_2O_3 from first principles calculations

Elena Bazhenova, Karoliina Honkala*

Nanoscience Center, Department of Chemistry, University of Jyväskylä, P.O. Box 35, FI-40014 Jyväskylä, Finland

A R T I C L E   I N F O

Article history:
Received 5 October 2016
Received in revised form 27 January 2017
Accepted 3 February 2017
Available online 21 February 2017

Keywords:
Density functional theory
Mn_2O_3
Bulk
Fe dopants

A B S T R A C T

Manganese oxides, particularly Mn_2O_3, have demonstrated great potential for oxygen carrier materials in chemical looping applications. The application of these materials in the industrial scale is hindered by thermodynamic restrictions related to the reoxidation process. This disadvantage can be overcome by doping the oxide with a guest cation. Iron is one of the most promising dopants, but the atomic-level understanding of its effects on the properties of α-Mn_2O_3 is incomplete. Herein, we report a systematic GGA+U study of the bulk properties and reducibility of $Fe_xMn_{2-x}O_3$ ($0 \le x \le 2$) as a function of Fe dopant concentration. In particular, we focus on a representative set of 20 models with different Fe content, generated by screening several thousand structures. Our results indicate that substitution of Mn atoms with Fe stabilizes $Fe_xMn_{2-x}O_3$, which is visible through negative values of doping energies, decreasing oxide formation energies, and higher oxygen vacancy formation energies with increasing Fe concentration. Similar to Fe, the presence of an oxygen vacancy increases the band gap in the major spin channel of $Fe_xMn_{2-x}O_3$. Oxygen transport in $Fe_xMn_{2-x}O_3$ is found to depend on Fe content and distribution in the lattice. All in all, our findings provide atomic-level insight into the properties of $Fe_xMn_{2-x}O_3$ and generally agree with experimental observations. Obtained information can be applied to investigate the reactivity of $Fe_xMn_{2-x}O_3$.

1. Introduction

Chemical Looping (CL) processes are an appealing technology offering an effective and versatile reduction-oxidation scheme to convert carbonaceous fuels into heat, electricity, or hydrogen in large scale applications providing CO_2 capture at a low cost [1–3]. Requisite oxygen is supplied by a solid oxygen carrier, which acts as a redox catalyst. During the reduction step, the carrier donates oxygen, which is then used to oxidize a given reactant, leading to the formation of oxygen deficient carrier materials. In the following healing step, the carrier is filled in again with oxygen. This reloading takes place under oxygen atmosphere in a physically separate reactor.

The future success in CL applications depends sensitively on oxygen carrier materials, and thus significant research efforts have been put forward to design and develop suitable materials. The desirable properties of promising oxygen carrier materials include high oxygen-carrying capacity, high fuel conversion, good redox reactivity, and high thermal stability. Experimentally, Cu, Ni, Fe, Mn, and Co-based oxides [4] are found to be most promising carrier materials for different CL applications [5,6]. These primary, active, transition metal oxides are typically supported by an inert oxide such as ZrO_2, Al_2O_3, and SiO_2 [4]. Cu and Mn oxides demonstrate high activity for CL combustion processes [4] and Fe oxide, on the other hand, is found to be a promising redox catalyst for methane partial oxidation [3]. The usage of pure manganese oxides is thermodynamically limited due to problematic reoxidation of the oxide under operating temperature [7]. In other words, oxygen release takes place easily, but the reoxidation of the reduced oxide is challenging. To improve oxygen uptake, Mn oxide is typically mixed with another oxide. This has been done for the following combinations of host and guest cations: Mn/Mg[8], Mn/Ni [9], Mn/Si [10,11], and Mn/Fe oxides [12–18]. Among the studied systems, Mn/Fe oxide has been found to be the most promising compromise between oxygen release and reoxidation [12–18].

While the properties of different oxygen carrier materials have been extensively explored experimentally, computational studies are scarce and they mainly focus on the properties of surfaces and supported clusters. Density functional theory calculations (DFT) employing both periodic [19,20] and cluster models [21] have been carried out for CO oxidation to CO_2 on α-Fe_2O_3. The calculations

---

* Corresponding author.
E-mail addresses: karoliina.honkala@jyu.fi, karoliina.honkala@gmail.com (K. Honkala).

http://dx.doi.org/10.1016/j.cattod.2017.02.004
0920-5861/© 2017 Elsevier B.V. All rights reserved.

show that on the surface of α-Fe_2O_3 CO prefers to adsorb on the O-top site forming CO_2 with lattice oxygen desorbing then with an activation energy of less than 20 kJ/mol. The carrier-support interactions have been explored computationally for CO oxidation at a MgO-supported Fe_2O_3 cluster [21]. The calculations show that the support increases the average Fe—O bond distance activating Fe_2O_3 for oxygen release. The computed activation energy for CO oxidation is about 158 kJ/mol lower on the supported cluster compared to a free-standing cluster. Improved CO adsorption has also been observed for Fe_2O_3 clusters supported on ZnO_2 and Al_2O_3 surfaces [22–24]. Another example of a computational study on carrier-support interactions deals with CuO/ZrO_2 and focuses on sintering of Cu-oxide clusters and CO oxidation on the supported cluster [25]. According to calculations, the strong interaction between the CuO cluster and the ZrO_2 support hinders the migration of the cluster while simultaneously activating it towards CO oxidation. The activation energy for CO oxidation decreases from 139 kJ/mol on the unsupported cluster to 76 kJ/mol on the supported one. Recently, chemical looping reforming of methane on α-Fe_2O_3(001) has been studied via DFT calculations [26]. On the stoichiometric α-Fe_2O_3 (001) surface, methane adsorption is found to be weak and the adsorption energy of the methane-derived radicals increases with decreasing number of H atoms. On the reduced surface, methane adsorption is even weaker than on the stoichiometric surface, while the adsorption strength of radicals significantly increases. Overall, the addition of an oxygen vacancy and stronger adsorption of radicals are proposed to promote oxidation of methane [26] and thus to improve the performance of α-Fe_2O_3 as an oxygen carrier.

Computational studies on α-Mn_2O_3 mainly focus on the bulk properties of the oxide, in particular the electronic structure and magnetic ordering [27,28]. Surface activity is considered for oxygen reduction and water oxidation [29]. The combined experimental and DFT investigation demonstrates the great potential of α-Mn_2O_3 as a bifunctional catalyst for oxygen reduction and oxygen evolution reactions, where the ability of an Mn ion to change its oxidation state from +3 to +4 is particularly important for the overall catalytic performance. Moreover, it is found that pH and the applied potential impact on the stability of an oxide surface, and Mn_2O_3 experiences a phase transition under the certain conditions.

Although α-Fe_2O_3 and α-Mn_2O_3 have been previously addressed, computational studies on β-Fe_2O_3 and Fe-doped α-Mn_2O_3 are not available in the literature. However, atomic-level understanding how Fe dopants affect structural and electronic properties and the reducibility of α-Mn_2O_3 would help to elucidate their behavior in CL applications.

Herein, we present a systematic evaluation of bulk properties and reducibility of $Fe_xMn_{2-x}O_3$ oxides as a function of their chemical composition employing density functional theory calculations. We begin with screening several thousand structures and selecting a representative set of models for the doped oxides. For each selected structure, doping energy, oxide formation energy, and electronic and magnetic structures are carefully examined. Finally, we study the energy of vacancy formation and oxygen diffusion to address efficiency of redox kinetics, which is the central property of an oxygen carrier.

2. Methods and models

2.1. Computational details

Periodic electronic structure calculations were performed using the grid-based projector augmented plane wave approach, as implemented in GPAW 0.10.0 [30–32]. Wave functions were represented on a uniform real-space grid with the spacing of 0.16 Å. Within the GGA+U formalism, Perdew-Burke-Ernzerhof (PBE) exchange-correlation functional [33] was used together with the Hubbard U correction [34,35] of 4 eV [36] for both Mn and Fe atoms to account for strong on-site Coulomb interaction. Main results were tested against different U values for Mn and Fe d-orbitals. We found that changes in U values introduce small variations to calculated quantities such as band gaps and vacancy formation energies, but the overall trends remain the same (see Supplementary material, Section 1). The Fermi smearing with the width of 0.2 eV was applied and all the calculations were performed at the Γ-point, which has been previously demonstrated to be a valid approach [37]. Atomic positions were always relaxed until maximum residual force was below 0.035 eV/Å. The impact of a tighter convergence criteria was found to be minor to the computed energy differences. The diffusion barriers were determined employing the Nudged Elastic Band (NEB) method [38] with the total number of images being 7.

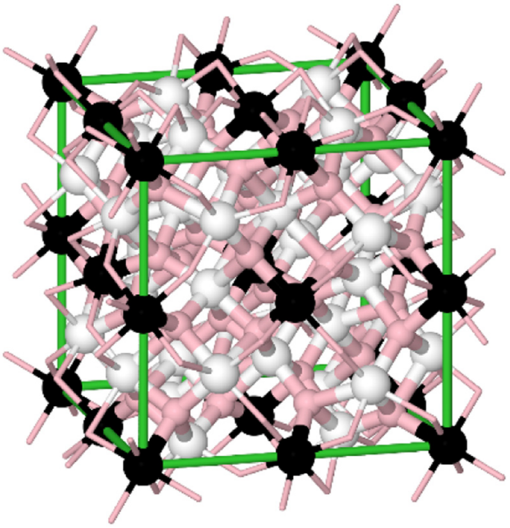

Fig. 1. The computational cell of the bixbyite structure of α-Mn_2O_3. Color indicates different Wyckoff positions: metal atoms at positions A are colored black, metal atoms at positions D are given in white, and oxygen atoms in positions E are represented in pink. (For interpretation of the references to color in this figure legend, the reader is referred to the web version of this article.)

2.2. Structures of pure and mixed oxides

Manganese (III) oxide exists in two forms, namely α-Mn_2O_3 and γ-Mn_2O_3, which differ from each other in the symmetry of crystal. More importantly, the γ-form dominates at low temperatures while α-Mn_2O_3 is more stable at high-temperature, CL, conditions [39,40]. In addition, the α-form can be further stabilized by replacing Mn cations in the lattice with Fe [39]. Therefore, we employed α-Mn_2O_3 throughout the current study. The α-Mn_2O_3 bulk belongs to the Ia-3 space group and exhibits the bixbyite structure (Fig. 1), where Mn atoms occupy 8 Wyckoff positions A and 24 Wyckoff positions D, while O atoms occupy 48 Wyckoff positions E [41]. Note, that metal atoms occupying different Wyckoff positions differ in local symmetry operations [42] (atoms in position A have higher symmetry than atoms in position D), but have the same coordination and surroundings. Iron (III) oxide features a variety of different crystal structures: α-Fe_2O_3 (hematite) with space group R-3c, β-Fe_2O_3 with space group Ia-3, γ-Fe_2O_3 (maghemite) with space group $P2_13$, and ε-Fe_2O_3 with space group $Pna2_1$. Even though the most common form Fe_2O_3 is α, the β-form is of a particular interest to the current study, as it is isomorphic to α-Mn_2O_3.

The atomic structure of $Fe_xMn_{2-x}O_3$ oxide is very complex and depends on the preparation method, ambient conditions, and